NOTICE: This material may be protected by Copyright Law (TITLE 18 U.S. Code)
and is not to be used for any purpose other than private study, scholarship, or research.

NAVIGATION: *Journal of The Institute of Navigation*
Vol. 35, No. 2, Summer 1988
Printed in U.S.A.

Autonomous GPS Integrity Monitoring Using the Pseudorange Residual

BRADFORD W. PARKINSON and PENINA AXELRAD

Stanford University, Stanford, California
Received January 1988
Revised May 1988

ABSTRACT

The use of GPS for navigation-critical applications such as aircraft nonprecision approach or harbor and river crossings requires the navigation data to be both extremely accurate and extremely reliable. This paper describes a method for autonomous GPS satellite failure detection and isolation (D/I). The test statistic for the D/I algorithm is the range residual parameter for six or more satellites in view. Based on experiments conducted at Stanford, nominal carrier-aided pseudorange measurement errors are modeled as Gaussian random variables with mean in the range from −5 m to +5 m and standard deviation of 0.4 m. The theoretical statistical distribution of the range residual is given. Monte Carlo simulations present results of applying the algorithm to measurement sets containing a biased measurement. With a 100 m biased measurement present, successful detection is achieved 99.9 percent of the time, and successful D/I is achieved 72.2 percent of the time. The user is always aware when isolation is not possible. User positioning errors resulting from application of the algorithm are always the same or better than with the all-in-view solution.

INTRODUCTION

As the GPS nears its operational capability, there is growing interest within the potential user community in applying it to a variety of high-precision navigation problems, such as river and harbor navigation, aircraft nonprecision approach, real-time or kinematic surveying, and spacecraft orbit determination. These applications not only require the highly precise navigation data afforded by GPS, but require them all the time. Thus arises the need for effective methods for monitoring GPS integrity. Significant research efforts addressing integrity issues have been going on since about 1980 [1].

The objective of all integrity monitoring techniques is to ensure the accuracy and reliability of a navigation system during critical mission phases. Receiver autonomous integrity monitoring (RAIM) is the name coined by the FAA for methods that achieve this objective by relying on redundant GPS satellite measurements [2]. Three subsets of the RAIM methodology can be identified.

Solution monitoring is currently receiving the most attention in the GPS integrity literature. This truly is the issue of primary concern to a large class of users, for example, an aircraft about to execute a nonprecision approach.

NOTICE: This material may be protected by Copyright Law (TITLE 18 U.S. Code)
and is not to be used for any purpose other than private study, scholarship, or research.

NOTICE: This material may be protected by Copyright Law (TITLE 18 U.S. Code)
and is not to be used for any purpose other than private study, scholarship, or research.

Solution monitoring methods set a 2-D or 3-D radial "protection limit" that indicates the position offset the user can tolerate without considering a navigation system failure [2].

Measurement monitoring is concerned with identifying an actual problem with a GPS satellite measurement. It is similar to the type of monitoring done at the ground-based stations; however, the autonomous algorithm does not have access to outside information.

Failure isolation is merely an extension of measurement monitoring. In this case, the objective is not only to detect a satellite failure, but also to identify which satellite has failed. Once this has been accomplished, the user can take the appropriate action to improve the navigation information.

Numerous algorithms for autonomous monitoring have been suggested by researchers at various organizations, such as The MITRE Corporation [3–5], Iowa State University [6–8], Navstar Systems Development [9], and Stanford University [10–12]. The majority can be described as "snapshot" approaches because they use a single set of GPS measurements collected simultaneously. The researchers at Iowa State University have also investigated the use of Kalman filtering as an alternative to the snapshot solution.

The technique developed at Stanford is geared toward measurement detection and isolation (D/I). It is based on a single all-in-view solution for detection, and subset solutions for failed satellite isolation. The test statistic, known as the residual parameter, is the normalized root sum square of the pseudorange measurement residuals.

EXPERIMENTAL DETERMINATION OF RANGING ERROR STRUCTURE

An accurate model of both nominal and degraded measurement errors is essential for the design and evaluation of any integrity verification scheme. Systematic experiments aimed at uncovering the pseudorange measurement error structure were conducted at Stanford using a state-of-the-art GPS surveying receiver. The following sections describe the experiments and the results obtained.

Equipment

The GPS receiver used for the ranging error tests is a Trimble Navigation 4000S Model Surveying Receiver. This five-channel set tracks up to five satellites and provides the option of using Doppler information in addition to the raw pseudorange measurements [13]. A Trimble micro-strip antenna was mounted atop the High Energy Physics Lab at Stanford, at a reference point surveyed by Geophysical Survey Inc. to submeter-level accuracy [14]. This type of antenna has been found to reduce the occurrence of multipath interference. An IBM PC XT was used for control of the receiver using Trimble data collection software, and for data storage and analysis. Information from each of the five channels was stored every 15 s.

Technique

The 4000S has the capability to report the predicted range and pseudorange measurements to each of five satellites in view. The pseudorange measurement

NOTICE: This material may be protected by Copyright Law (TITLE 18 U.S. Code)
and is not to be used for any purpose other than private study, scholarship, or research.

NOTICE: This material may be protected by Copyright Law (TITLE 18 U.S. Code)
and is not to be used for any purpose other than private study, scholarship, or research.

is based on the signal transit time from satellite to user, corrected for satellite clock errors, ionospheric and tropospheric delays, relativistic effects, satellite clock offset, group delay, etc. [13]. The measurement may also be adjusted using integrated Doppler if the Doppler-aiding option on the receiver is selected. This pseudorange measurement contains errors due to the satellite and user clock model inaccuracies, propagation link delay model errors, multipath interference, receiver noise, and interchannel biases.

The predicted range, which is called "distance" in the Trimble reference manual, is based on the receiver's current estimate of position and the satellite ephemeris data provided in the navigation message. Normally, the receiver estimates its position using the combination of four satellites in view with the lowest geometric dilution-of-precision (GDOP) value. To investigate the independent measurement errors, we suppressed this function of the receiver and provided it with the known antenna location: 37:25.6861 N, 122:10.4690 W, 6.94 m. The only significant error in the calculated distance is due to the satellite ephemeris. Note that a correction to the measurements was applied to account for earth rotation.

The true ranging errors were then isolated by computing the difference between the pseudorange, ρ, and the distance plus clock offset, $d + b$:

$$\rho = d_0 + b - \varepsilon_c - \varepsilon_p - \varepsilon_m - \varepsilon_r \tag{1}$$

$$d = d_0 + \varepsilon_e \tag{2}$$

$$\begin{aligned} \varepsilon &= d + b - \rho \\ &= \varepsilon_e + \varepsilon_c + \varepsilon_p + \varepsilon_m + \varepsilon_r \end{aligned} \tag{3}$$

where

ε_e = ephemeris errors
ε_c = user clock bias estimation errors − uncorrected satellite clock errors
ε_p = propagation link errors, i.e., uncorrected ionospheric and tropospheric delays
ε_m = multipath errors
ε_r = receiver errors

Experimental Results

Pseudorange measurements were collected on various days in August and September, 1987. The results are classified into three categories:

1) Nominal Doppler-Aided are Doppler-aided pseudorange measurements with no loss of signal lock.
2) Nominal Unaided are pseudorange measurements based on code only, satellite above 15 deg elevation, health status good.
3) Degraded are all other types of measurements, including aided measurements during repeated loss of signal lock, measurements made to satellites near the horizon, and measurements made to satellites that have failed for any reason.

The objective of the integrity verification algorithm is to identify the presence of degraded measurements (Category 3) within a set of nominal measurements.

Tables 1 and 2 summarize the results for Category 1 and 2 measurements,

NOTICE: This material may be protected by Copyright Law (TITLE 18 U.S. Code)
and is not to be used for any purpose other than private study, scholarship, or research.

NOTICE: This material may be protected by Copyright Law (TITLE 18 U.S. Code)
and is not to be used for any purpose other than private study, scholarship, or research.

Table 1—Nominal Aided Range Error Statistics (m)

DATE	SV03		SV06		SV09		SV11		SV12		SV13	
	mean	σ	mean	σ	mean	σ	mean	σ	mean	σ	mean	σ
AUG 19	3.37	0.42	3.90	0.39	*	*	−4.38	0.16	−2.38	0.17	−0.52	0.15
AUG 26a	*	*	0.08	0.16	−2.79	0.38	−0.14	0.12	0.66	0.15	2.19	0.18
AUG 26b	−2.65	0.33	*	*	−1.54	0.43	*	*	2.01	0.23	2.18	0.15
SEP 1b	1.38	0.36	*	*	0.77	0.16	−3.92	0.11	−2.63	0.21	4.39	0.32
SEP 2a	*	*	0.59	0.16	0.95	0.11	−1.42	0.23	−2.71	0.16	2.59	0.13
SEP 2b	4.13	0.27	*	*	−0.26	0.40	*	*	−2.84	0.39	−1.03	0.59
SEP 9b	0.16	0.18	*	*	3.12	0.18	−3.02	0.33	−2.74	0.28	2.48	0.22
AVERAGE	1.28	0.31	1.52	0.24	0.04	0.28	−2.58	0.19	−1.52	0.23	1.75	0.25

Note: The sum of the means for each session should be approximately 0 m because a bias common to all measurements is absorbed in the clock estimate.

Table 2—Nominal Unaided Range Error Statistics (m)

DATE	SV03		SV06		SV09		SV11		SV12		SV13	
	mean	σ	mean	σ	mean	σ	mean	σ	mean	σ	mean	σ
AUG 17	2.06	2.56	−2.30	2.29	*	*	−1.08	1.84	1.77	1.69	−0.45	1.28
SEP 5a	*	*	3.18	1.93	−0.06	1.29	−2.42	1.70	−1.64	1.66	0.94	1.29
SEP 5b	−1.39	2.07	*	*	2.21	1.85	−2.10	3.24	−0.74	1.85	2.01	2.11
SEP 10a	*	*	3.29	1.96	−0.69	1.34	−1.48	1.67	−1.96	1.66	0.83	1.50
SEP 10b	1.63	1.91	*	*	1.94	1.88	−2.04	3.47	−1.23	1.83	−0.30	2.03
AVERAGE	0.77	2.18	1.39	2.06	0.85	1.59	−1.82	2.38	−0.76	1.74	0.61	1.64

Note: The sum of the means for each session should be approximately 0 m because a bias common to all measurements is absorbed in the clock estimate.

NOTICE: This material may be protected by Copyright Law (TITLE 18 U.S. Code)
and is not to be used for any purpose other than private study, scholarship, or research.

NOTICE: This material may be protected by Copyright Law (TITLE 18 U.S. Code)
and is not to be used for any purpose other than private study, scholarship, or research.

respectively. We originally anticipated that SV8 would serve as a good example of a failed satellite since it is operating on a quartz crystal clock. However, the experimentally determined ranging errors to SV8 were not substantially different from typical nominal unaided measurements.

These results led us to formulate the following measurement error models:

1) Nominal Doppler-Aided—normally distributed random variable with mean ranging from −5 m to +5 m and standard deviation of 0.4 m.
2) Nominal Unaided—normally distributed random variable with mean ranging from −5 m to +5 m and standard deviation of 4.0 m.
3) Degraded—normally distributed with standard deviation of 0.4 m for aided and 4.0 m for unaided, and a mean greater than 5 m.

The objective of the integrity verification algorithm, then, is to reliably detect measurements for which the bias is greater than the nominal mean measurement error. We wish to emphasize that errors which may be intentionally introduced by selective availability are *not* modeled in this study.

RANGE RESIDUAL PARAMETER

This section describes the range residual parameter, r, which is used as the test statistic for failure D/I. Background theory on the method for calculating this parameter and its theoretical statistical distribution is presented in the Appendix. Only the results from the Appendix are summarized here.

We assume that the user forms a least squares estimate of position and clock offset based on pseudorange measurements to all satellites in view. The range residual for a particular satellite is defined to be the difference between its pseudorange and the range computed based on these estimates of position and clock offset. The range residual parameter, r, is then defined as follows:

$$r \equiv \frac{s\sigma}{\sqrt{n-4}} \tag{4}$$

where

s = RSS of the normalized range residuals to the n satellites;
σ = standard deviation of the pseudorange errors;
n = number of satellites in view.

The principal advantage of the parameter r as a test statistic is that its theoretical distribution is relatively insensitive to the user/satellite geometry. The Appendix shows that s^2 has a χ^2 distribution with $n-4$ degrees of freedom when the measurement errors are normally distributed with zero mean. The distribution is modified to a *noncentral* χ^2 distribution if the measurement errors are biased. In this case, the distribution is affected more strongly by geometry through the noncentrality parameter.

It is important to keep in mind that the actual value of r depends on both the pseudorange measurement errors and the particular user/satellite geometry. The theoretical distribution gives only the statistical probability of obtaining certain values.

Knowledge of the theoretical distribution of the range residual provides important insight into how well it will serve as the test statistic. However,

NOTICE: This material may be protected by Copyright Law (TITLE 18 U.S. Code)
and is not to be used for any purpose other than private study, scholarship, or research.

NOTICE: This material may be protected by Copyright Law (TITLE 18 U.S. Code)
and is not to be used for any purpose other than private study, scholarship, or research.

actual implementation of the algorithm requires numerical values for D/I thresholds of the test statistic. These are best determined by Monte Carlo simulation results. Appropriate thresholds may then be selected based on requirements for probability of false alarm and missed detection.

DETECTION/ISOLATION PROCEDURE

The D/I procedure is extremely straightforward. The five steps are given below, followed by a discussion of how threshold values for the test statistics can be selected.

Procedure

The user may perform integrity checking and failed satellite isolation as follows:

1) Compute the residual parameter, r, using all satellites in view (six or more) from equation (4).
2) If r is less than the detection threshold, r_D, assume that all satellites are operating properly, and the integrity check has been completed. If r is greater than r_D, a failure has been detected.
3) If a failure is detected in step (2), compute the residual parameters, $r^1, r^2, \ldots, r^n$, for the n subsets of $n-1$ satellites.
4) If one of the r^i's is less than the isolation threshold, r_I, and all others are larger than r_I, identify the satellite omitted from the i'th subset as the failed one. If two or more of the residual parameters are below the threshold, the failed satellite cannot be isolated.
5) If a failed satellite is detected and isolated, use the navigation solution formed by omitting the failed one. If a failed satellite is detected, but cannot be isolated, use the all-in-view solution if necessary, but recognize that the positioning accuracy is degraded.

Threshold Selection

The most effective way to select the threshold values, r_D and r_I, is based on Monte Carlo simulation results. The difficulty in applying statistical theory to the actual selection of threshold values of the test statistic is due to the fact that the GPS pseudorange measurements actually have a slowly varying component. Measurement biases significantly affect the expected distribution, but of course the user has no way of determining their values.

Users should select D/I thresholds based on requirements for false alarm and missed detection. In this section, we present extensive Monte Carlo computer simulation results that facilitate the choice of appropriate threshold values.

The simulation program assumes a 3-plane, uniform 24-satellite constellation, and a surface user with elevation mask angle of 7.5 deg. Range errors are modeled as normally distributed, with $\sigma = 0.4$ m, and means ranging from -5 m to $+5$ m with uniform probability. Note that we did *not* model errors that may be caused by selective availability. Every 15 min, 100 sets of measurements are generated using this range error model. In most cases, the user is located at San Francisco Airport. During the 24 h simulations, 16,600 data

NOTICE: This material may be protected by Copyright Law (TITLE 18 U.S. Code)
and is not to be used for any purpose other than private study, scholarship, or research.

NOTICE: This material may be protected by Copyright Law (TITLE 18 U.S. Code)
and is not to be used for any purpose other than private study, scholarship, or research.

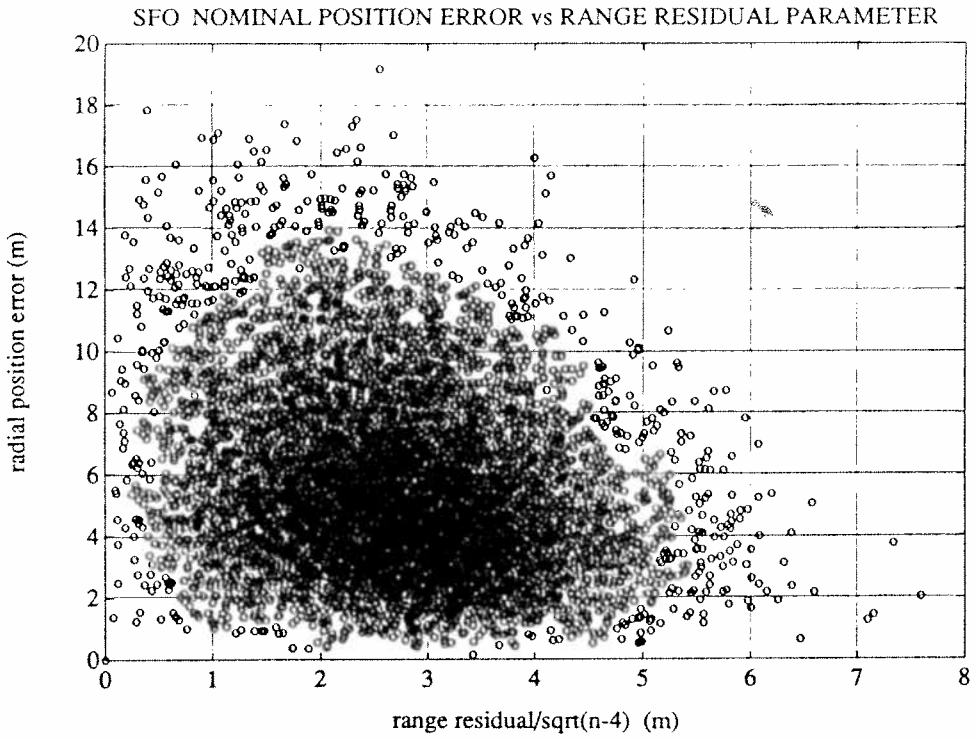

Fig. 1—Nominal Position Error vs Range Residual Parameter for San Francisco—All-in-View Solution

points are generated. A number of runs performed for the Chicago area produced almost identical results.

Figure 1 shows the radial position errors vs r for nominal measurement errors at San Francisco (SFO) over a 24 h period. It is clear that the residual parameter is always less than 8 m, and the radial position error is less than 20 m.

Figure 2 illustrates position errors vs r at SFO when a bias of 50 m is added to one of the satellite ranges. At each time step, 100 runs are performed with each of the satellites in view in turn designated as the failed one. For example, with six satellites in view at time 0, 600 data points are generated. If eight satellites are visible 15 min later, 800 data points are generated at that time. Table 3 gives the ranges of the residual parameter and positioning errors for nominal measurements and biases of 25 m, 50 m, and 100 m.

Figure 3 shows the probability of false alarm and missed detection as a function of detection threshold for several satellite biases. The probability of false alarm (P_{FA}) is the likelihood that a satellite failure will be declared when all measurements are actually in the nominal range. The probability of missed detection (P_{MD}) for a given bias is the likelihood that no failure will be detected when one of the measurements is actually biased by the specified amount. For example, if the detection threshold is set at 8 m, satellite biases of 100 m will *always* be detected; 50 m biases will be detected 99.9 percent of the time, 37.5 m biases 98.5 percent of the time, and 25 m biases 75 percent of the time.

NOTICE: This material may be protected by Copyright Law (TITLE 18 U.S. Code)
and is not to be used for any purpose other than private study, scholarship, or research.

NOTICE: This material may be protected by Copyright Law (TITLE 18 U.S. Code)
and is not to be used for any purpose other than private study, scholarship, or research.

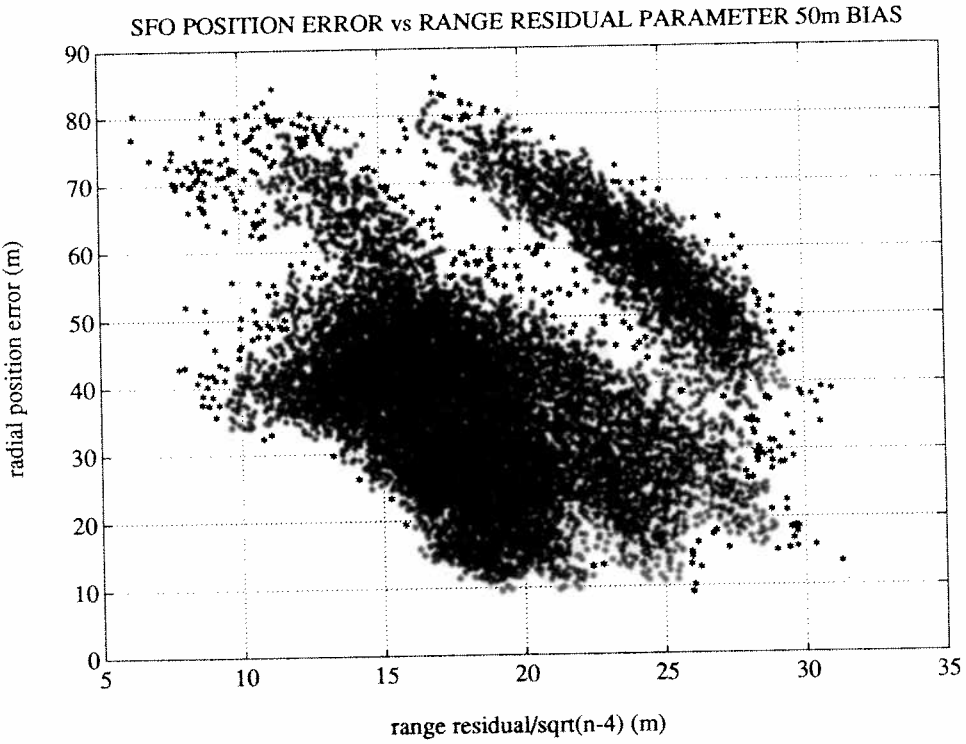

Fig. 2—Position Error vs Range Residual Parameter with 50 m Biased Measurement

Table 3—Range of Residual Parameter and Position Error

Bias (m)	Residual Parameter (m)	Position Error (m)
0	0–8	0–20
100	15–60	20–160
50	6–32	9–90
25	2–18	3–48

If a failure is detected, the user computes the residual parameter for each subset of $n-1$ satellites. Figure 4 illustrates the position errors and residual parameters for the subset containing only nominal satellite measurements. Notice that the residual parameter for these nominal subsets is still always less than 10 m. Figures 5 and 6 show the position error vs r for all $n-1$ subsets that contain a failed satellite with bias errors of 100 m and 50 m, respectively. For the 100 m bias error, 94.7 percent of the subset range residuals are greater than 10 m. For the 50 m bias error, 86.8 percent of the subset range residuals are greater than 10 m.

If only one of the subset solutions has a residual parameter less than the isolation threshold, it must be the one consisting of only nominal measurements. Thus the user can successfully remove the biased satellite from the measurement set. If two or more subsets are below the threshold, at least one will contain the failed satellite. The user will then realize that failure isolation

NOTICE: This material may be protected by Copyright Law (TITLE 18 U.S. Code)
and is not to be used for any purpose other than private study, scholarship, or research.

NOTICE: This material may be protected by Copyright Law (TITLE 18 U.S. Code)
and is not to be used for any purpose other than private study, scholarship, or research.

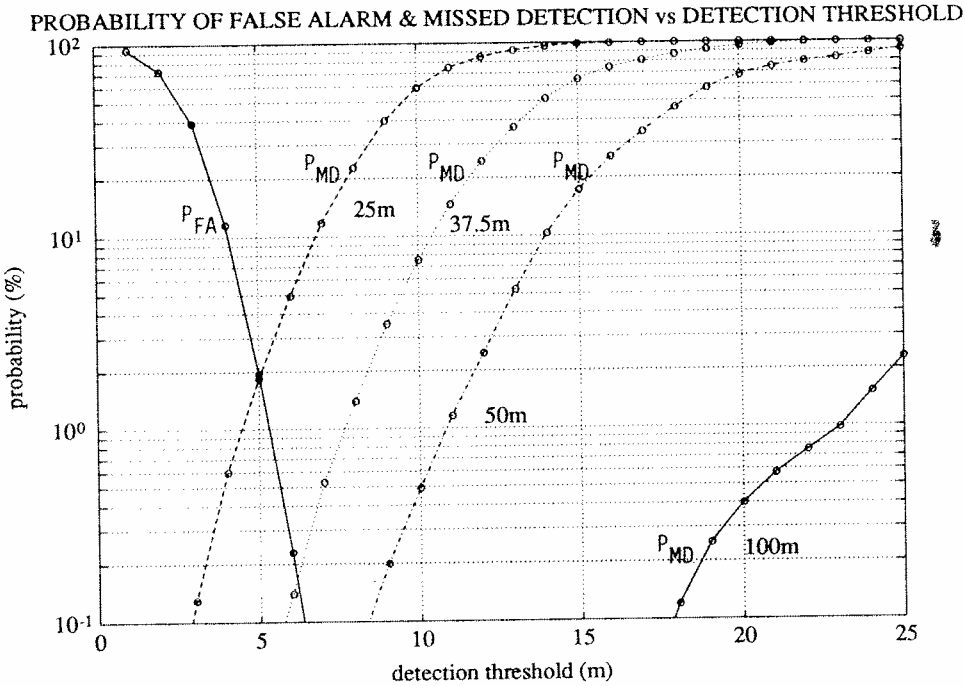

Fig. 3—Probability of False Alarm and Missed Detection vs Detection Threshold for Biases of 25 m, 37.5 m, 50 m, and 100 m

is not possible. Thus the algorithm ensures that a healthy satellite will never be mistakenly removed from the navigation solution.

Table 4 summarizes the Monte Carlo simulation results when the algorithm is implemented with $r_D = 8$ m, and $r_I = 10$ m. The probabilities of missed detection (MD), successful D/I (OK), and successful detection without isolation (NI) are given.

The important question that remains is, "What impact does this process have on the user's position error?" This issue is addressed in the discussion below.

DISCUSSION

From the figures in the previous section, we determined that a detection threshold value of $r_D = 8$ m would produce good results in terms of low probability of false alarm and missed detection. An isolation threshold of $r_I = 10$ m produced fairly good results in terms of users' ability to remove the biased measurement. When successful D/I is accomplished, users are 99.95 percent sure that their position errors will be smaller than 25 m (Figure 4). When a failure is detected but cannot be isolated, users know that their navigation solution is not reliable, but can do nothing to improve it.

The primary objective of a large group of GPS users is to minimize the error in the overall navigation solution. While the presence of a biased pseudorange measurement will in general degrade the accuracy of the navigation solution, the user/satellite geometry may be such that even a large bias will have only a minor effect on position accuracy. In addition, if the subset geometry without

NOTICE: This material may be protected by Copyright Law (TITLE 18 U.S. Code)
and is not to be used for any purpose other than private study, scholarship, or research.

NOTICE: This material may be protected by Copyright Law (TITLE 18 U.S. Code)
and is not to be used for any purpose other than private study, scholarship, or research.

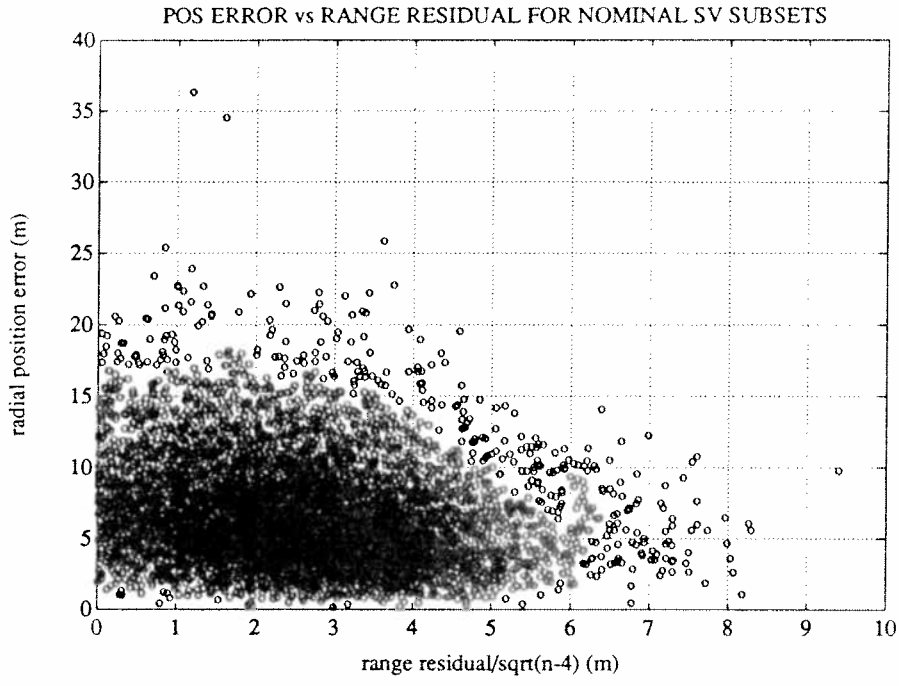

Fig. 4—Position Error vs Range Residual for SV Subsets That Do Not Include the Biased Satellite

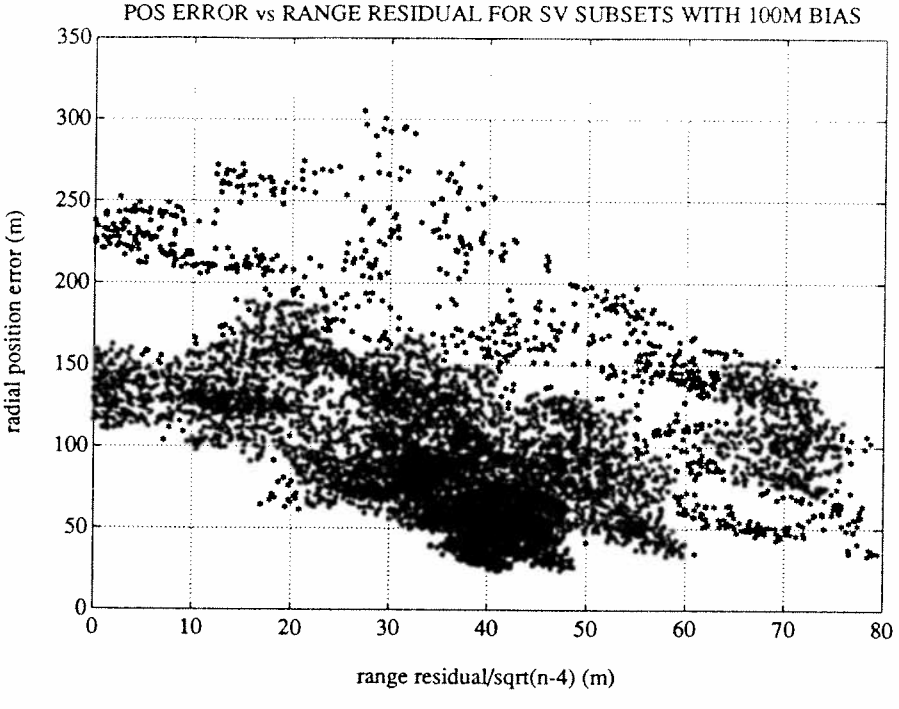

Fig. 5—Position Error vs Range Residual for Subsets Including SV with 100 m Bias

NOTICE: This material may be protected by Copyright Law (TITLE 18 U.S. Code)
and is not to be used for any purpose other than private study, scholarship, or research.

NOTICE: This material may be protected by Copyright Law (TITLE 18 U.S. Code)
and is not to be used for any purpose other than private study, scholarship, or research.

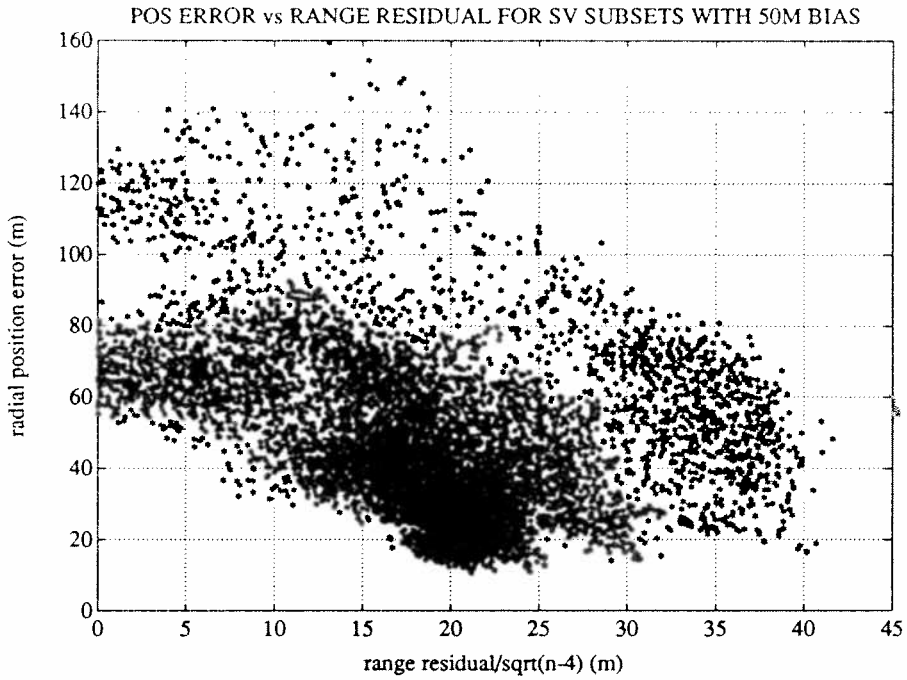

Fig. 6—Position Error vs Range Residual for Subsets Including SV with 50 m Bias

Table 4—Probability of Detection and Isolation with r_D = 8 m, r_I = 10 m

BIAS (m)	PROBABILITY (%)		
	Missed Detection	Bias Detected and Isolated	Bias Detected Not Isolated
100	0.0	72.2	27.8
50	0.06	50.5	49.5
37.5	1.3	34.2	64.5
25	23.2	6.4	70.4

the failed satellite is extremely weak, positioning errors may be worse if the biased measurement is not used in forming the navigation solution.

In Figure 1 we see that, given the experimentally determined nominal error model, the magnitude of the positioning errors using all satellites in view is less than 20 m. If one of the measurements has a bias of 100 m, that measurement will be detected. If the measurement bias is less than 100 m, there is a finite probability that the measurement will not be detected. Figures 7 and 8 show the probability of incurring various radial position errors when biases of 50 m and 25 m are not detected. Results are given for detection threshold values of 4 m to 12 m. The sum of the probabilities indicated on each of the curves represents the probability of missed detection for the particular bias and detection threshold. Notice that although the probability of missed detection for a bias of 25 m is rather large, the resulting position errors are generally within the range of nominal navigation errors.

If the satellite is isolated and the biased pseudorange is removed from the

NOTICE: This material may be protected by Copyright Law (TITLE 18 U.S. Code)
and is not to be used for any purpose other than private study, scholarship, or research.

NOTICE: This material may be protected by Copyright Law (TITLE 18 U.S. Code)
and is not to be used for any purpose other than private study, scholarship, or research.

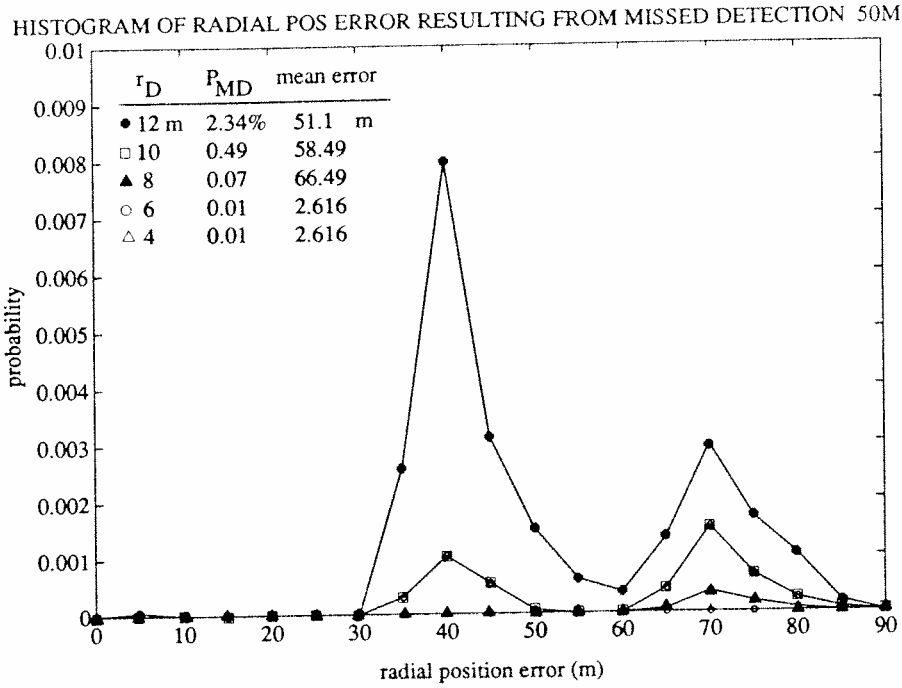

Fig. 7—Distribution of Radial Errors When a 50 m Bias Is NOT Detected for Detection Thresholds r_D = 4, 6, 8, 10, 12 m

measurement set, the resulting position errors are less than 25 m 99.95 percent of the time, as seen in Figure 4. If the satellite cannot be isolated, the user will have to compute position from measurements to all the satellites, resulting in positioning errors of up to 160 m for a 100 m bias and 90 m for a 50 m bias, as in Table 3. The important aspect of this is that the user will realize that the position solution is not reliable.

Figures 9 through 11 compare the distribution of the positioning errors that result from an all-in-view solution and the integrity checking algorithm solution, in the presence of one measurement biased by 100 m, 50 m, and 25 m, respectively. Each chart represents the results of 16,600 Monte Carlo runs. The curve marked "ALL" shows the probability density for positioning errors that would be obtained by a user who formed an all-in-view solution and did no integrity checking. The area under this curve is equal to 1.0.

The integrity checking algorithm follows the previously described steps 1–5 to detect a satellite failure and to isolate the biased measurement if possible. If no bias is detected, there is a missed detection because in the simulation, one of the satellites is always biased. In this case, the user forms a solution based on all-in-view and does not know that something is amiss. If a failure is detected but cannot be isolated, the all-in-view solution is again used. In this situation, however, the user is aware that the navigation solution is unreliable. If isolation is successful, the failed satellite is removed from the measurement set used to form the solution. The three curves labeled MD, NI, and OK show the conditional probability density functions for these three possible outcomes of the

NOTICE: This material may be protected by Copyright Law (TITLE 18 U.S. Code)
and is not to be used for any purpose other than private study, scholarship, or research.

NOTICE: This material may be protected by Copyright Law (TITLE 18 U.S. Code)
and is not to be used for any purpose other than private study, scholarship, or research.

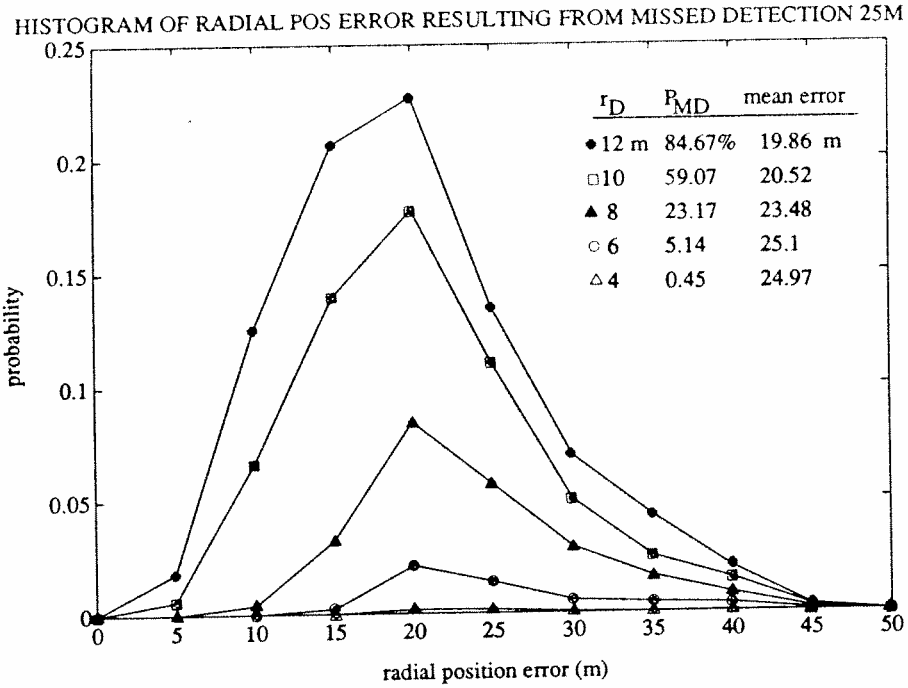

Fig. 8—Distribution of Radial Position Errors When a 25 m Bias Is NOT Detected for Detection Thresholds r_D = 4, 6, 8, 10, 12 m

D/I algorithm. The sum of the areas under the three curves is equal to 1.0. It is clear that the algorithm has significantly reduced the likelihood of large navigation errors. In addition, when large errors are unavoidable, the user is aware that the solution is unreliable.

Lowering the user's elevation mask angle can significantly improve performance by increasing the number of satellites that are visible. Figure 12 illustrates the probability density of the errors for a user with a 0 deg mask angle in the presence of a 50 m bias. By comparing this with the results shown in Figure 10 for a user with 7.5 deg elevation mask angle, we can quickly notice the reduction in mean error and the increase in the number of successful detections and isolations. The user can detect and isolate 78.6 percent of the time with a 0 deg mask, as compared to only 50.5 percent of the time with a 7.5 deg mask.

CONCLUSIONS

We have presented a practical new approach to GPS integrity checking. Three key subjects have been addressed: 1) experimental determination of the measurement error structure, 2) theoretical distribution of the range residual parameter, and 3) a practical means of implementing a D/I scheme based on this parameter. Each of these topics was essential in developing a sound methodology for solving the problem of GPS navigation reliability.

For users with carrier tracking C/A code receivers, such as the Trimble 4000S, the results presented here are directly applicable. The error structure of a

NOTICE: This material may be protected by Copyright Law (TITLE 18 U.S. Code)
and is not to be used for any purpose other than private study, scholarship, or research.

NOTICE: This material may be protected by Copyright Law (TITLE 18 U.S. Code)
and is not to be used for any purpose other than private study, scholarship, or research.

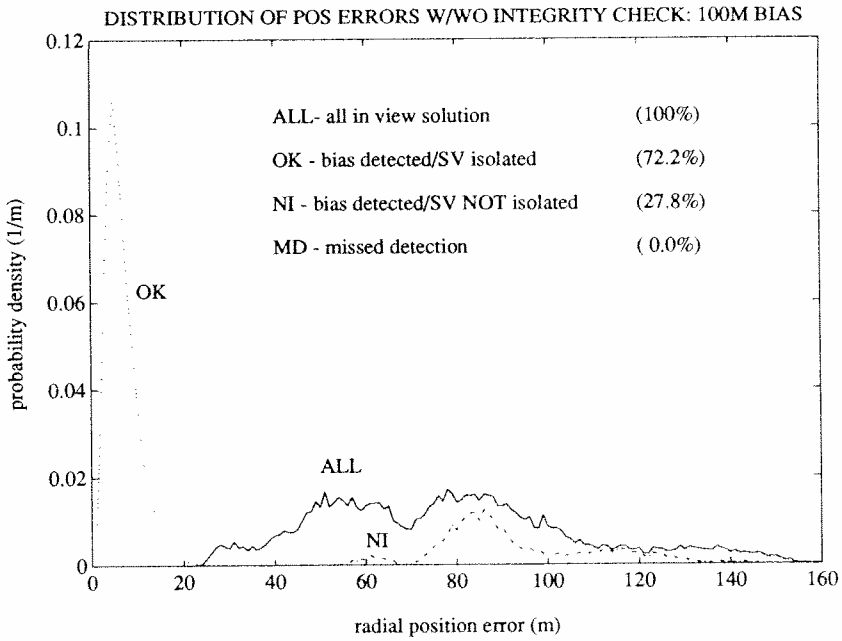

Fig. 9—Probability Density Function for Radial Position Errors from All-in-View Solution, and Conditional Probability Density Functions for Radial Position Errors from Possible Outcomes of Integrity Checking Algorithm. One SV Biased by 100 m

different class of receiver will produce different results; however, the framework for selecting detection and isolation thresholds and for evaluating the algorithm performance is identical to that presented here. For this reason, it is important for receiver manufacturers and users to clearly understand the characteristics of the measurement errors. Error test statistics must be compiled for the environmental conditions and vehicle dynamics in which the system is expected to perform.

The algorithm described is a snapshot approach to integrity monitoring. Under certain circumstances, the performance may be improved by averaging the test statistic over several measurement times. This would be particularly useful for a code-only receiver, in which the measurement errors are dominated by white noise. In the case of a carrier tracking receiver, we have found the measurement errors to be slowly varying in nature, with a low level of high-frequency noise. In this situation, it is not likely that time averaging will cause much improvement.

The range residual-based integrity verification method is reliable and easy to implement as part of a navigation software package. It will never degrade a user's solution and can frequently eliminate biased measurements, allowing a user to continue on a critical mission phase. When isolation is not possible, a user may have to postpone navigation-critical maneuvers. The only dangerous condition arises from the unlikely occurrence of a missed detection. Further studies may produce a method for predicting when missed detections are more likely, based on subset solution geometry [15]. By implementing the integrity

NOTICE: This material may be protected by Copyright Law (TITLE 18 U.S. Code)
and is not to be used for any purpose other than private study, scholarship, or research.

NOTICE: This material may be protected by Copyright Law (TITLE 18 U.S. Code)
and is not to be used for any purpose other than private study, scholarship, or research.

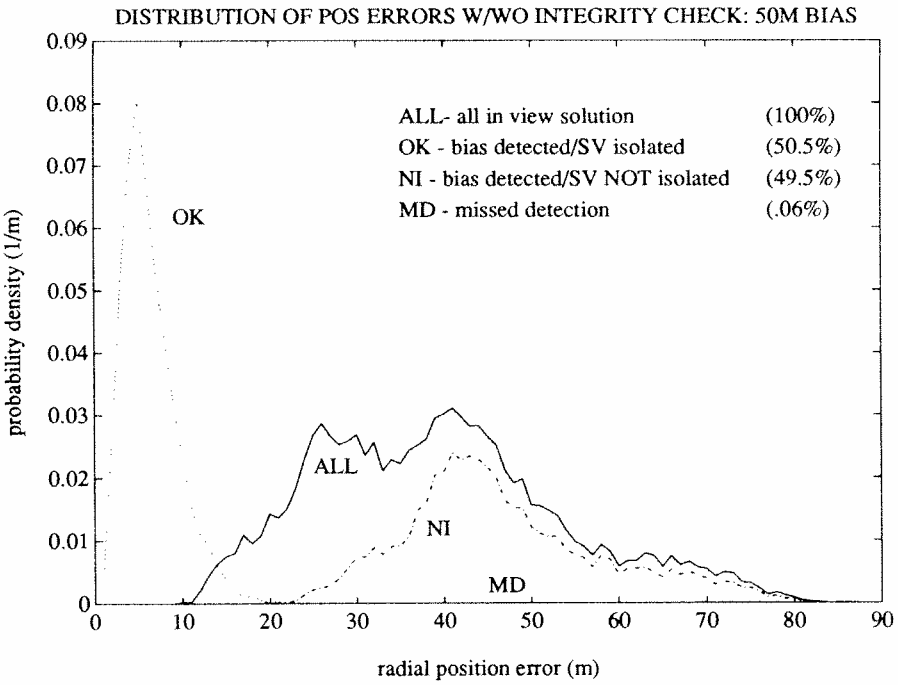

Fig. 10—Probability Density Functions for Radial Position Errors. One SV Biased by 50 m

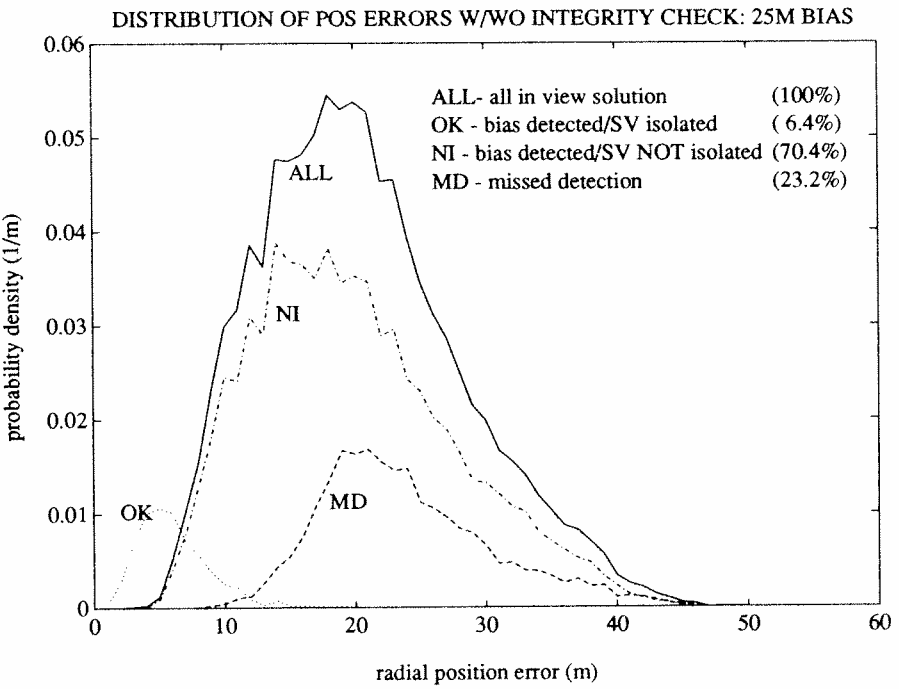

Fig. 11—Probability Density Functions for Radial Position Errors. One SV Biased by 25 m

NOTICE: This material may be protected by Copyright Law (TITLE 18 U.S. Code)
and is not to be used for any purpose other than private study, scholarship, or research.

NOTICE: This material may be protected by Copyright Law (TITLE 18 U.S. Code)
and is not to be used for any purpose other than private study, scholarship, or research.

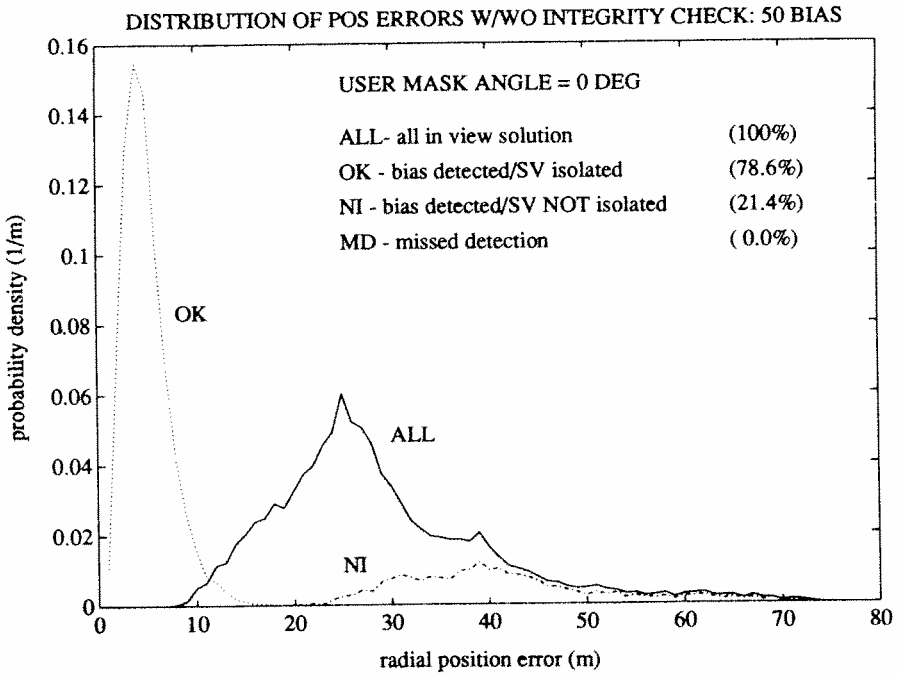

Fig. 12—Probability Density Functions for Radial Position Errors. One SV Biased by 50 m. User Mask Angle 0.0 Deg (9700 Data Points)

check, the user will have an accurate measure of the reliability of the navigation solution.

REFERENCES

1. Shively, C. A., *Review of Methods for GPS Integrity,* The MITRE Corporation, MP-87W22, March 1988.
2. Kalafus, R. M. and Chin, G. Y., *Performance Measures of Receiver-Autonomous GPS Integrity Monitoring,* Proceedings of the ION National Technical Meeting, Santa Barbara, 1988.
3. Lee, Y. C., *Analysis of Range and Position Comparison Methods as Means to Provide GPS Integrity in the User Receiver,* Proceedings of ION 42nd Annual Meeting, Seattle, 1986.
4. Lee, Y. C., The MITRE Corporation Memorandum W46-M4380, 25 February 1986.
5. Lee, Y. C., The MITRE Corporation Memorandum W46-M4422, 4 April 1986.
6. Brown, R. G. and Hwang, P. Y. C., *GPS Failure Detection by Autonomous Means Within the Cockpit,* Proceedings of ION 42nd Annual Meeting, Seattle, 1986.
7. Brown, R. G. and McBurney, P. W., *Self-Contained GPS Integrity Check Using Maximum Solution Separation,* NAVIGATION, Journal of the Institute of Navigation, Vol. 35, No. 1, Spring 1988.
8. McBurney, P. W. and Brown, R. G., *Self-Contained GPS Failure Detection: The Kalman Filter Approach,* Proceedings of the ION Satellite Division Technical Meeting, Colorado Springs, 1987.
9. Brown, A. K., *Receiver Autonomous Integrity Monitoring Using a 24-Satellite GPS Constellation,* Proceedings of the ION Satellite Division Technical Meeting, Colorado Springs, 1987.

NOTICE: This material may be protected by Copyright Law (TITLE 18 U.S. Code)
and is not to be used for any purpose other than private study, scholarship, or research.

NOTICE: This material may be protected by Copyright Law (TITLE 18 U.S. Code)
and is not to be used for any purpose other than private study, scholarship, or research.

10. Parkinson, B. W. and Axelrad, P., *Simplified GPS Integrity Checking with Multiple Satellites,* Proceedings of the ION National Technical Meeting, Dayton, 1987.
11. Parkinson, B. W. and Axelrad, P., *A Basis for the Development of Operational Algorithms for Simplified GPS Integrity Checking,* Proceedings of the ION Satellite Division Technical Meeting, Colorado Springs, 1987.
12. Parkinson, B. W. and Axelrad, P., *A Practical Algorithm for Autonomous Integrity Verification Using the Pseudo Range Residual,* Proceedings of the ION National Technical Meeting, Santa Barbara, 1988.
13. Trimble Navigation, *User's Guide to Operation of the 4000S Surveying Receiver,* 1987.
14. Geophysical Survey Inc., *Preliminary Survey Report for TAU Corporation,* August, 1987.
15. McBurney, P. W., private communication, January, 1988.
16. Strang, G., *Linear Algebra and Its Applications,* Academic Press Inc., New York, 1980.
17. Cook, R. D. and Weisberg, S., *Residuals and Influence in Regression,* Chapman and Hall, 1982.
18. Kshirsagar, A. M., *A Course in Linear Models,* Marcel Dekker Inc., 1983.
19. Patnaik, P. B., *The Non-Central χ^2- and F-Distributions and Their Applications,* Biometrika, Vol. 36, 1949.
20. Kendall, M. G. and Stuart, A., *The Advanced Theory of Statistics,* Vol. 2, Hafner Publishing Co., 1973.

NOTICE: This material may be protected by Copyright Law (TITLE 18 U.S. Code)
and is not to be used for any purpose other than private study, scholarship, or research.

NOTICE: This material may be protected by Copyright Law (TITLE 18 U.S. Code)
and is not to be used for any purpose other than private study, scholarship, or research.

APPENDIX: BACKGROUND THEORY

This Appendix provides background on the least squares estimation process necessary for GPS integrity checking and describes the distribution of the range residual parameter used as a test statistic in the D/I algorithm.

Least Squares Estimation in GPS

The pseudorange measurement equation is given by,

$$\rho_i = D_i - [\mathbf{e}_i^T \; 1]\,\mathbf{x} - \varepsilon_i \tag{A-1}$$

where

- ρ_i = pseudorange measurement to SV_i;
- D_i = projection of the vector from the earth center to SV_i onto the line of sight from the user to SV_i;
- $\mathbf{e}_i$ = unit vector along line of sight from user to SV_i;
- $\mathbf{x}$ = (4×1) matrix consisting of the vector from the earth center to the user and the user clock bias;
- ε_i = normally distributed measurement error $\sim N(\mu_i,\sigma_i)$.

The pseudorange measurements to the n satellites in view are combined in the following matrix equation:

$$\mathbf{y} \equiv (\mathbf{D} - \boldsymbol{\rho}) = \mathbf{G}\mathbf{x} + \boldsymbol{\varepsilon} \tag{A-2}$$

where

$$\mathbf{D} = \begin{bmatrix} D_i \\ \cdot \\ \cdot \\ D_n \end{bmatrix}, \boldsymbol{\rho} = \begin{bmatrix} \rho_i \\ \cdot \\ \cdot \\ \rho_n \end{bmatrix}, \mathbf{G} = \begin{bmatrix} \mathbf{e}_i^T \; 1 \\ \cdot \quad \cdot \\ \cdot \quad \cdot \\ \mathbf{e}_n^T \; 1 \end{bmatrix}, \boldsymbol{\varepsilon} = \begin{bmatrix} \varepsilon_i \\ \cdot \\ \cdot \\ \varepsilon_n \end{bmatrix}$$

The least squares estimate of $\mathbf{x}$, denoted by $\hat{\mathbf{x}}$, is then given by,

$$\hat{\mathbf{x}} \equiv (\mathbf{G}^T\mathbf{G})^{-1}\mathbf{G}^T\mathbf{y} \tag{A-3}$$

Based on $\hat{\mathbf{x}}$, an estimate of $\mathbf{y}$ can be formed:

$$\hat{\mathbf{y}} = \mathbf{G}\hat{\mathbf{x}} = \mathbf{P}\mathbf{y} \tag{A-4}$$

where

$$\mathbf{P} = \mathbf{G}(\mathbf{G}^T\mathbf{G})^{-1}\mathbf{G}^T$$

$\mathbf{P}$ is commonly referred to as the "projection matrix" or the "hat matrix" [16,17].

The matrix of range residual errors, $\hat{\boldsymbol{\varepsilon}}$, is the difference between the predicted

NOTICE: This material may be protected by Copyright Law (TITLE 18 U.S. Code)
and is not to be used for any purpose other than private study, scholarship, or research.

NOTICE: This material may be protected by Copyright Law (TITLE 18 U.S. Code)
and is not to be used for any purpose other than private study, scholarship, or research.

and measured ranges. This ends up being equivalent to the difference between $\mathbf{y}$ and $\hat{\mathbf{y}}$.

$$\hat{\boldsymbol{\varepsilon}} \equiv \underbrace{(\mathbf{D}-\mathbf{G}\hat{\mathbf{x}})}_{\{predicted\}} - \underbrace{\boldsymbol{\rho}}_{\{measured\}} \tag{A-5}$$

$$\begin{aligned}\hat{\boldsymbol{\varepsilon}} &= \mathbf{D} - \boldsymbol{\rho} - \mathbf{G}\hat{\mathbf{x}} \\ &= \mathbf{y} - \hat{\mathbf{y}} \\ &= (\mathbf{I}-\mathbf{P})\,\mathbf{y} = (\mathbf{I}-\mathbf{P})\boldsymbol{\varepsilon}\end{aligned} \tag{A-6}$$

The matrices $\mathbf{P}$ and $(\mathbf{I}-\mathbf{P})$ are $(n\times n)$ idempotent matrices with

$\text{trace}(\mathbf{P}) = \text{rank}(\mathbf{P}) = \text{rank}(\mathbf{G}) = 4$
$\text{trace}(\mathbf{I}-\mathbf{P}) = n-4$ [18].

An orthogonal transformation, $\mathbf{K}$, can be found, which diagonalizes $(\mathbf{I}-\mathbf{P})$ to an $n\times n$ matrix with $n-4$ diagonal elements equal to "1" and 4 diagonal elements equal to "0." The sum of the squares of the range residual errors (SSE) can be expressed as [18]:

$$\begin{aligned}\text{SSE} &= \hat{\boldsymbol{\varepsilon}}^{\mathrm{T}}\hat{\boldsymbol{\varepsilon}} = \text{trace}(\hat{\boldsymbol{\varepsilon}}\hat{\boldsymbol{\varepsilon}}^{\mathrm{T}}) \\ &= \boldsymbol{\varepsilon}^{\mathrm{T}}(\mathbf{I}-\mathbf{P})\boldsymbol{\varepsilon} = \text{trace}\{(\mathbf{I}-\mathbf{P})\boldsymbol{\varepsilon}\boldsymbol{\varepsilon}^{\mathrm{T}}(\mathbf{I}-\mathbf{P})\}\end{aligned} \tag{A-7}$$

$$\begin{aligned}\text{SSE} &= \mathbf{u}^{\mathrm{T}}\text{diag}(1,\ldots,1,0,\ldots,0)\mathbf{u} \\ &= u_1^2 + \cdots + u_{n-4}^2\end{aligned} \tag{A-8}$$

where

$\mathbf{u} = \mathbf{K}\boldsymbol{\varepsilon}$.

Distribution of the Error Sum of Squares

The sum of the squares of the range residual errors normalized by the standard deviation of the measurement errors is defined as $s^2 = \text{SSE}/\sigma^2$.

If the measurement errors are independent, normally distributed random variables, with mean 0 and standard deviation σ, i.e., $\varepsilon_i \sim N(0,\sigma)$, then the u_i's are also normally distributed with the same mean and standard deviation, *and* $u_1, \ldots, u_{n-4}$ are independent. Thus s^2 has a chi-square distribution with $n-4$ degrees of freedom (DOF).

If instead the errors are independent, normally distributed random variables with *nonzero* means, $\varepsilon_i \sim N(\mu_i,\sigma)$, then s^2 has a *noncentral* chi-square distribution with $n-4$ DOF, and noncentrality parameter,

$$\lambda = \frac{\boldsymbol{\mu}^{\mathrm{T}}(\mathbf{I}-\mathbf{P})\boldsymbol{\mu}}{\sigma^2} \tag{A-9}$$

where

$$\boldsymbol{\mu}^{\mathrm{T}} = [\mu_1 \ldots \mu_n]$$

The noncentral chi-square probability density function is given by,

$$f(s^2) = \frac{e^{-(s^2+\lambda)/2}}{2^{(n-4)/2}} \sum_{j=0}^{\infty} \frac{(s^2)^{(n-4)/2+j-1}\,\lambda^j}{\Gamma\left(\frac{n-4}{2}+j\right)\cdot 2^{2j}\cdot j!} \tag{A-10}$$

which reduces to the standard chi-square density function for $\lambda = 0$ [19, 20].

NOTICE: This material may be protected by Copyright Law (TITLE 18 U.S. Code)
and is not to be used for any purpose other than private study, scholarship, or research.

NOTICE: This material may be protected by Copyright Law (TITLE 18 U.S. Code)
and is not to be used for any purpose other than private study, scholarship, or research.

In his 1949 article in *Biometrika*, Patnaik describes several approximations to the noncentral chi-square distribution that vary in their computational requirements and accuracy. For the integrity verification algorithm, his "first" approximation is sufficient. In this model, the density function of the noncentral chi-square variable, s^2, with $(n-4)$ degrees of freedom and noncentrality parameter λ, is approximated by,

$$f(s^2) \approx \rho f_{\chi^2}(s^2/\rho) \tag{A-11}$$

which is assumed to have a chi-square distribution with ν degrees of freedom, where,

$$\rho = 1 + \frac{\lambda}{(n-4)+\lambda}$$

$$\nu = (n-4) + \frac{\lambda^2}{(n-4)+2\lambda}$$

Note that ν, the DOF in the approximation, is not necessarily an integer. The corresponding probability distribution is obtained by numerical integration of the density function given by equation (A11), or interpolation in tables.

Range Residual Parameter

The range residual parameter, r, is then defined as follows:

$$r \equiv \sqrt{\frac{\hat{\epsilon}^T\hat{\epsilon}}{n-4}} = \sqrt{\frac{s^2\sigma^2}{n-4}} \tag{A12}$$

This parameter is used as the test statistic in the D/I algorithm described earlier.

NOTICE: This material may be protected by Copyright Law (TITLE 18 U.S. Code)
and is not to be used for any purpose other than private study, scholarship, or research.